Adeno-associated virus-mediated gene therapy in a patient with Canavan disease using dual routes of administration and immune modulation

Manuela Corti,[1,15] Barry J. Byrne,[1,15] Dominic J. Gessler,[2,3] Grace Thompson,[4] Samantha Norman,[1] Jenna Lammers,[1] Kirsten E. Coleman,[1] Cristina Liberati,[1] Melissa E. Elder,[1,5] Maria L. Escolar,[6] Ibrahim S. Tuna,[7] Clementina Mesaros,[8,9] Gary I. Kleiner,[10] Deborah S. Barbouth,[11] Heather L. Gray-Edwards,[2,12] Nathalie Clement,[1] Brian D. Cleaver,[1] and Guangping Gao[2,13,14]

[1]Powell Gene Therapy Center, Department of Pediatrics, College of Medicine, University of Florida, Gainesville, FL, USA; [2]Horae Gene Therapy Center, University of Massachusetts Medical School, Worcester, MA, USA; [3]Department of Neurosurgery, University of Minnesota Medical School, Minneapolis, MN, USA; [4]Department of Pediatric Surgery, College of Medicine, University of Florida, Gainesville, FL, USA; [5]University of Florida Health Shands Children's Hospital, Gainesville, FL, USA; [6]Department of Pediatrics, School of Medicine, University of Pittsburgh, Pittsburgh, PA, USA; [7]Department of Radiology, College of Medicine, University of Florida, Gainesville, FL, USA; [8]Penn Medicine/Children's Hospital of Philadelphia Center of Excellence in Friedreich's Ataxia, University of Pennsylvania, Philadelphia, PA, USA; [9]Center of Excellence in Environmental Toxicology, Department of Systems Pharmacology and Translational Therapeutics, Perelman School of Medicine, University of Pennsylvania, Philadelphia, PA, USA; [10]Department of Pediatrics, Miller School of Medicine, University of Miami, Miami, FL, USA; [11]Division of Clinical and Translational Genetics, Department of Human Genetics, Miller School of Medicine, University of Miami, Miami, FL, USA; [12]Department of Radiology, University of Massachusetts Medical School, Worcester, MA, USA; [13]Li Weibo Institute for Rare Diseases Research, University of Massachusetts Medical School, Worcester, MA, USA; [14]Department of Microbiology and Physiological Systems, University of Massachusetts Medical School, Worcester, MA, USA

Gene replacement therapy is a rational therapeutic strategy and clinical intervention for neurodegenerative disorders like Canavan disease, a leukodystrophy caused by biallelic mutations in the aspartoacylase (*ASPA*) gene. We aimed to investigate whether simultaneous intravenous (i.v.) and intracerebroventricular (i.c.v.) administration of rAAV9-CB6-ASPA provides a safe and effective therapeutic strategy in an open-label, individual-patient, expanded-access trial for Canavan disease. Immunomodulation was given prophylactically prior to adeno-associated virus (AAV) treatment to prevent an immune response to ASPA or the vector capsid. The patient served as his own control, and change from baseline was assessed by clinical pathology tests, vector genomes in the blood, antibodies against ASPA and AAV capsids, levels of cerebrospinal fluid (CSF) *N*-acetylaspartate (NAA), brain water content and morphology, clinical status, and motor function tests. Two years post treatment, the patient's white matter myelination had increased, motor function was improved, and he remained free of typical severe epilepsy. NAA level was reduced at 3 months and remained stable up to 4 years post treatment. Immunomodulation prior to AAV exposure enables repeat dosing and has prevented an anti-transgene immune response. Dual-route administration of gene therapy may improve treatment outcomes.

INTRODUCTION

Canavan disease is a childhood leukodystrophy caused by mutations in the aspartoacylase (ASPA) gene.[1] In oligodendrocytes, ASPA con- verts *N*-acetylaspartate (NAA), an abundant amino acid involved in brain development and homeostasis, into acetate and aspartate.[2,3] Deficiency of ASPA results in excess NAA, oligodendrocyte dysfunc- tion, prominent spongiform changes, and absence of myelin.[4]

Canavan disease is a progressive disease that usually begins during the first few months of life.[2] Early clinical signs include macrocephaly, lack of head control, and hypotonia, which results in floppiness and delayed motor milestones, such as independent sitting and walking. Subse- quently, the hypotonia progresses to joint stiffness and spasticity. The untreated natural history includes intractable epilepsy, with increasing seizures by age 10, and death often occurs by adolescence.[2,5,6]

Currently, there is no treatment for Canavan disease.[2] Gene therapy to replace the defective *ASPA* gene is the most rational treatment. In 1996 and 1998, the first two clinical trials of gene transfer therapy for Canavan disease demonstrated that intraventricular administration of a nonviral vector containing the *ASPA* gene was safe, but clinical improvements were limited and variable between individuals.[7,8] Since then, recombinant adeno-associated virus (rAAV) vectors have become the preferred gene therapy platform for targeting central ner- vous system (CNS) disease.[9] In one study, 13 patients with Canavan

disease were treated with multisite intraparenchymal injections of an AAV serotype 2 (AAV2) vector containing the human *ASPA* gene and were followed for more than a decade with no safety findings.[3] However, the reduction in NAA levels was modest and not uniform throughout the brain. These findings suggest that a different route of administration or a different AAV serotype could target neurons and oligodendrocytes more specifically and achieve broader vector distribution and normalization of NAA levels throughout the brain.

Over the last decade, an rAAV-based gene therapy developed at the University of Massachusetts (UMass; Worcester, MA; Dr. Gao's laboratory) has demonstrated that intravenous (i.v.) and intracerebroventricular (i.c.v.) delivery prevent Canavan disease and extend survival in a mouse model.[10,11] Further optimization of this gene therapy not only completely prevented Canavan disease in mice but also rescued mice after the onset of symptoms.[12,13] The preclinical studies have also led to a gene therapy that is currently being evaluated in an open-label phase 1/2 clinical study (ClinicalTrials.gov: NCT04998396).

Here, we describe the safety and effectiveness of simultaneous i.v. and i.c.v. injections of the abovementioned AAV serotype 9 (AAV9)-based gene replacement therapy in a 2-year-old child with Canavan disease. AAV9 was selected because of its tropism for the brain.[14] On the basis of prior studies of gene therapy for Pompe disease, a glycogen storage disorder caused by mutations in the a-glucosidase gene, immune modulation was used before, during, and after AAV administration to prevent immune responses against the vector or transgene.[15]

Study design

This study was an open-label, individual-patient, expanded-access trial of a simultaneous single i.v. and i.c.v. administration of rAAV9-CB6-ASPA in a child with Canavan disease. The study participant received immunosuppression prior to AAV therapy to prevent reaction to the ASPA gene product and vector capsid protein.

The study participant's guardian provided written informed consent prior to enrollment. The study was approved by the University of Florida (UF; Gainesville, FL, USA) institutional review board.

Case report

At the time of diagnosis, the study participant was a 6-month-old boy with a history of irritability, reflux, developmental delay, and visual problems. He underwent neurological and genetic evaluation with brain magnetic resonance imaging (MRI) and magnetic resonance spectroscopy (MRS), which showed abnormal myelination and elevated NAA consistent with leukodystrophy. The diagnosis of Canavan disease was confirmed based on biallelic *ASPA* mutations (Tyr231X and Glu285Ala).

At 9 months of age, the patient was enrolled in an observational longitudinal study at UF in preparation for a subsequent treatment study as a collaboration between UF (Dr. Byrne's laboratory) and UMass

(Dr. Gao's laboratory). Nonclinical investigational new drug-enabling studies were performed at UF. Upon approval and parental consent, the patient (22 months of age) was enrolled in an individual patient-expanded access trial at UF to receive investigational AAV9-*ASPA* gene replacement therapy (open label).

Study assessments

Adverse events (AEs) were graded according to the National Cancer Institute Common Terminology Criteria for Adverse Events (version 4). Laboratory analyses included blood, urine, and cerebrospinal fluid (CSF). Total anti-AAV9 immunoglobin G (IgG) and IgM and anti-ASPA IgG levels in serum were evaluated by enzyme-linked immunosorbent assays.

Quantitative polymerase chain reaction (qPCR) was used to quantify vector biodistribution (vector genome copy number) in blood samples. MRI and DTI (Siemens) were performed to assess brain morphology and white matter tract formation, respectively. Fractional anisotropy in the patient's brain was compared with mean values from 400 individuals without Canavan disease between birth and 3 years of age (data provided by Dr. Maria Escolar, University of Pittsburgh, Pittsburgh, PA, USA). NAA levels in CSF samples and the brain were measured by mass spectrometry and proton MRS (Siemens), respectively. The patient also underwent a visual exam and a battery of neurodevelopmental assessment tests, including the Bayley Scales of Infant and Toddler Development,[16] Children's Hospital of Philadelphia Infant Test of Neuromuscular Disorders (CHOP-INTEND),[17] Motor Function Measure Scale – Short Form (MFM-20),[18] and Gross Motor Function Measure 88 (GMFM-88).[19]

RESULTS

Safety

No AEs related to the study agent were reported. Three AEs related to the study procedures occurred (a rash around the eyes related to rituximab infusion, emesis after prednisolone administration, and a transient CSF leak at the surgical site during ventriculostomy catheter placement). All AEs are listed in Table 1. Clinical laboratory results, including gamma-glutamyl transferase (GGT), aspartate aminotransferase (AST), alanine aminotransferase (ALT), platelets, alkaline phosphatase (AP), and bilirubin, are listed in Table 2. None of the clinical laboratory results changed significantly from baseline during the study.

Treatment outcomes

The patient was discharged 1 day after AAV administration by the i.v. and i.c.v. routes. More than 2 years post treatment, no new Canavan disease-related clinical events (such as onset of seizures or worsening of symptoms) or hospitalizations have occurred. The clinical findings are a dramatic departure from the natural history of Canavan disease and a reversal of the patient's disease trajectory.[5,6] Epilepsy, which is common in late-stage Canavan disease, has not been observed now up to 5 years post treatment.[5] Additionally, the natural history of Canavan disease is associated with early cortical blindness, which was

Table 1. Adverse events during treatment of a patient with Canavan disease with recombinant adeno-associated virus serotype 9-mediated human aspartoacylase (rAAV9-*hASPA*) gene transfer therapy

Event	Patient identifier	Date enrolled in study	Date of AE	Serious (Y/N)	Unanticipated (Y/N)	Related to study procedure (Y/N/cannot R/O)	Date reported to IRB[a]	Outcome
Red rash around eyes and minor swelling – reaction to first rituximab infusion	C-001	4/3/17	4/3/17	N	N	Y (related to rituximab infusion)	CR-2017	resolved
Emesis	C-001	4/3/17	4/4/17	N	Y	N	CR-2017	resolved
Bug bite on right foot	C-001	4/3/17	4/11/17	N	Y	N	CR-2017	resolved
Emesis following first dose of prednisolone oral solution; changed dosing plan to resolve AE	C-001	4/3/17	4/27/17	N	Y	Y (related to prednisolone administration)	CR-2017	resolved
Maculopapular rash on trunk, back, head, and thigh	C-001	4/3/17	5/24/17	N	Y	N	CR-2017	resolved
CSF leak and inflammation of surgical site	C-001	4/3/17	5/26/17	Y (SAE)	Y	Y	5/26/17	resolved
Rash (apparently drug related [linezolid]) during hospitalization for SAE	C-001	4/3/17	5/30/17	N	Y	N	CR-2017	resolved
Bug bite on left lateral neck area	C-001	4/3/17	6/5/17	N	Y	N	CR-2017	resolved
Gastric reflux	C-001	4/3/17	7/12/17	N	Y	N	CR-2017	ongoing
Febrile illness	C-001	4/3/17	9/12/17	N	Y	N	CR-2017	resolved
Vomiting	C-001	4/3/17	9/12/17	N	Y	N	CR-2017	resolved
Acute viral syndrome (coronavirus)	C-001	4/3/17	9/13/17	N	Y	N	CR-2017	resolved
Constipation	C-001	4/3/17	10/2/17	N	Y	N	CR-2017	resolved
Gastrointestinal tube removal (accidentally removed by mother)	C-001	4/3/17	10/11/17	N	Y	N	CR-2017	resolved
Fever	C-001	4/3/17	10/31/17	N	Y	N	CR-2017	resolved
IgG infusion inpatient	C-001	4/3/17	11/3/17	N	N	N	CR-2017	resolved
Hypogammaglobulinemia	C-001	4/3/17	11/3/17	N	Y	N	CR-2018	resolved
Fever	C-001	4/3/17	11/3/17	N	Y	N	CR-2018	resolved
Hypogammaglobulinemia	C-001	4/3/17	11/9/17	Y	Y	cannot R/O	11/9/17	resolved
Posterior humeral fracture	C-001	4/3/17	6/29/18	N	Y	N	CR-2018	ongoing

AE, adverse event; CR, continuing review; CSF, cerebrospinal fluid; IRB, institutional review board; R/O, rule out; SAE, serious AE; Y, yes; N, no.
[a]Date reported or reported with continuing review.

confirmed in the study participant prior to treatment based on persistent nystagmus and inability to fix and follow as well as limited response to his mother at 3 ft. Following treatment, nystagmus is resolved, and he is able to recognize his mother from a distance of over 6 ft. He has a left-gaze preference. Fundoscopic exam showed no evidence of retinal degeneration, and a full-field electroretinography (ERG) was normal versus age-matched responses for rods and cones.

MRI images compared with age-matched normal controls (Figures 1B and 1D), showed a diffuse decreased T1 signal (asterisk) as well as a diffuse increased T2 signal (asterisk) in our patient's baseline imaging, compatible with severe hypomyelination through the white matter. Similarly, on subsequent follow-up imaging, there is a more conspicuous and increased volume of T1 hyperintensity of the white matter (Figures 3A–3E), and T2 hypointensity of the white matter (Figures 2F–2J), particularly along the periventricular white matter and corpus callosum (Figure 2), was observed, which is suggestive of improved visualization of mature myelination on conventional MRI. Subsequent follow-up imaging, however, also demonstrated *ex vacuo* dilatation of the ventricles and CSF spaces, likely because of overall decreased

Table 2. Laboratory results for the study participant treated with AAV9-CB6-*hASPA* gene transfer therapy

Test	Reference range	Measurement time point			Days after AAV dosing											
		Consent	Baseline	AAV dosing	7	14	30	45	60	75	90	180	270	365	520	730
GGT	5–61 U/L	10	10	9	N/D	19	N/D	N/D	9	9	11	12	12	11	N/D	9
AST	0–30 IU/L	43	37	32	28	29	41	36	40	36	37	41	53	41	N/D	18
ALT	0–50 IU/L	24	17	15	18	20	28	22	22	22	24	31	31	22	N/D	25
Platelets	150–450 K/mL	244	349	181	293	362	212	311	219	297	212	216	244	210	187	232
AP	135–320 IU/L	196	172	156	154	126	137	188	222	230	223	238	194	207	N/D	213
Bilirubin	0–1.0 mg/dL	0.2	0.2	0.2	0.1	0.2	0.1	0.1	0.1	0.1	0.2	0.2	0.2	0.3	N/D	0.2

ALT, alanine aminotransferase; AP, alkaline phosphatase; AST, aspartate aminotransferase; GGT, gamma-glutamyl transferase; IU/L, international units per liter; K/mL, thousand per microliter; mg/dL, milligrams per deciliter; N/D, no data; U/L; units per liter.

parenchymal white matter volume and decreased white matter swelling and edema (Figure 2).

On days 90, 180, 365, and 730 and 4-year follow-up, NAA levels in the CSF were reduced approximately 80%, 80%, 85%, and 86% relative to baseline (Figure 3). Fractional anisotropy, which is a measure of white matter integrity based on the restriction of movement and orientation of water molecules, in the corticospinal tract and anterior corpus callosum progressively increased up to 2 years after treatment, indicating improved integrity of myelinated tracts (Figure 4). Concomitantly, motor development, which likely benefited from vision improvement, demonstrated improvement in four neurodevelopment scales (Figure 5). Vision was evaluated by two independent ophthalmologists, confirming improvement in visual function post treatment, representing a distinct change from the natural history of the disease. Vision was tested by clinical pediatric ophthalmology exam at the time of diagnosis and periodically for clinical follow-up at 15 months and 21 months of age, at baseline pre-treatment, as well as at 31 months (8 months post treatment) and 35 months (12 months post treatment). Age-appropriate testing included fixation and following, maternal face recognition, and grasping objects presented in distinct visual fields.

Immunogenicity

Recombinant AAV9-*hASPA* vector genomes persisted in the blood at very low levels for 2 years after treatment (Figure 6, top panel). During this time, anti-AAV9 IgG levels were unchanged from baseline and were four orders of magnitude lower than the levels in nonhuman primates that received the same dose of rAAV9-*hASPA* without immunomodulation (Figure 6, bottom panel). The increase in IgG levels on day 270 was most likely due to administration of i.v. Ig (IVIG) on day 180. Anti-AAV9 IgM levels increased slightly on day 14 but were still three orders of magnitude lower than the levels in nonhuman primate (NHP) controls without immunosuppression. Anti-ASPA antibody levels during the study did not differ from that at baseline.

DISCUSSION

This case study supports use of AAV-medicated gene therapy for Canavan disease using simultaneous i.v. and i.c.v. administration of an AAV9-*hASPA* vector combined with immunomodulation. Importantly, the treatment was safe, as evidenced by the lack of serious AEs related to the drug or immune responses during the study. In addition, use of immunomodulation prior to AAV exposure reduced antibody formation to the AAV capsid and transgene. In terms of efficacy, the findings demonstrated an approximately 80% reduction of NAA levels in the CSF up to 4 years post dosing and increased white matter myelination in the brain up to day 520 post dosing. Myelination, measured by fractoinal anisotropy (FA), improved in the bilateral corticospinal tracts and in the genu. No improvements were observed in the splenium. The different areas of the brain grow at different rates and in a spatial pattern. The overall higher values spatially across the brain are initially in the central white matter and lowest in the frontal white matter. The increases are faster in the occipital area and parietal white matter and slower in temporal and frontal areas. The corpus callosum growth starts from the center to the periphery and posterior
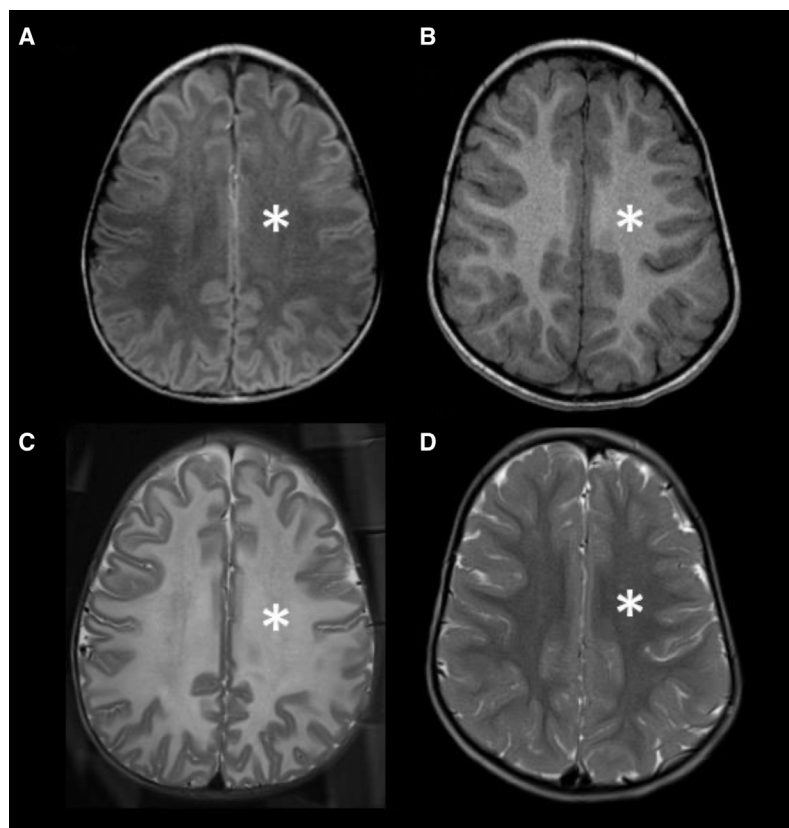
Figure 1. MRI of the brain of a 22-month-old patient with Canavan disease compared with an age-matched normal brain

T1W (A and B) and T2W (C and D) MRI of the brain of a 22-month-old patient with Canavan disease (A and C) and an age-matched normal brain MRI in a different patient (B and D). Compared with normal brain imaging (arrows in B and D), there is a diffuse decreased T1 signal (arrows in A) as well as a diffuse increased T2 signal (arrows in C) in our patient's baseline imaging, compatible with severe hypomyelination through the white matter.

to anterior. Myelination follows a similar pattern, with the splenium myelinating before the genu.[20–22] DTI is a measure of white matter tract integrity, so the FA value is influenced largely by the directionality of the myelinated bundles. Therefore, a disease affecting brain growth during the time when the splenium is developing (3–6 months of life) will injure this area more, as in the case of our patient, because there was treatment later when the genu develops, it was less affected. These changes corresponded to moderate improvements in motor development up to 2 years after treatment and improvements of visual function, as demonstrated by improvement in nystagmus and the ability to fix and follow at a distance as well as the ability to reach and grasp objects. Although the child remains below the developmental age of age-matched controls, all domains of the Bayley Scales of Infant and Toddler Development, except for fine movements, improved during the first 2 years post dosing, including cognitive, receptive, and expressive communications and gross motor function. The baseline cognitive evaluation (22-month-old) corresponded to the cognitive function of a 4-month year old. After treatment (41 months old), the cognitive level corresponded to that of an 8-month-old. Overall, the motor function of the child improved compared with baseline; however, the improvements were limited by increased tone, spasticity, and macrocephaly. This observation highlights the importance of early intervention. Altogether, these findings support the long-term, cumulative effectiveness of this approach to restore ASPA in the CNS.

Achieving therapeutic levels of many drugs, including gene therapy vectors, in the CNS via peripheral delivery is challenging because the blood-brain barrier (BBB) restricts entry of many molecules.[23] A viral vector that can cross the BBB, such as AAV9,[14,24] is critical to the success of this approach. However, achieving adequate CNS transduction via peripheral administration alone is a challenge in a disease that affects the periphery and CNS. High vector doses would be needed, which may increase the risk of immunogenicity and toxicity.[24,25]

Direct administration into the CNS (e.g., via intraparenchymal or i.c.v. routes) can bypass the BBB, but not all routes result in broad distribution.[24] Early attempts to treat Canavan disease using multisite intraparenchymal injections of AAV2-*ASPA* vectors only reduced NAA levels significantly in the periventricular and frontal regions of the brain but not other regions where ASPA is normally expressed (e.g., the cerebellum),[3] most likely because of the focal nature of the injections.[24,26] Broader distribution of AAV vectors can be achieved by delivery into the CSF.[24] For example, i.c.v. injection is an established and safe method of delivering therapeutics,[27] including AAV9, throughout the CNS.[24,27,28] However, i.c.v. administration alone may be insufficient to reach key brain regions affected by Canavan disease. A recent study of an investigational AAV9-*ASPA* gene transfer therapy for Canavan disease in macaques showed that i.v. administration, but not intrathecal or i.c.v. administration, resulted in vector transduction and ASPA expression in deep-brain structures affected by Canavan disease.[28] In addition, dual i.v. and i.c.v. administration of an AAV-based gene transfer therapy in a mouse model of Pompe disease outperformed either route of administration alone,[29] suggesting that a similar approach may be feasible for Canavan disease.

An important consideration for AAV gene therapy is the immune response against AAV capsid proteins. This response limits treatment to a single administration in eligible patients who do not have neutralizing antibodies against the vector.[26,30,31] In this study, rituximab and sirolimus reduced immune responses against AAV9 for 3 years, similar to previous studies that used rituximab to reduce anti-AAV antibody levels.[31] Long-term suppression of anti-AAV antibodies
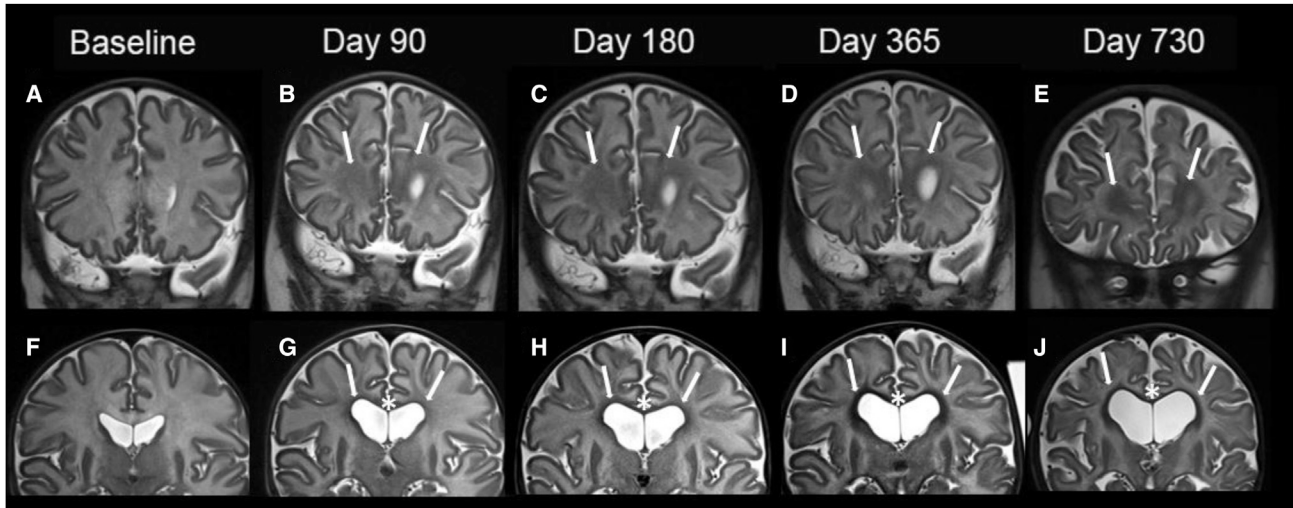
Figure 2. MRI of the brain of a patient with Canavan disease pre and post gene transfer therapy
Coronal T2W images of the brain at baseline (A and F) and 90-, 180-, 365-, and 730-day follow-up at the levels of anterior frontal white matter (A–E) and body of the corpus callosum (F–J). There is more conspicuous and increased volume of T2 (arrows) hypointensity on subsequent follow-up imaging after administration of rAAV9-hASPA, particularly in the periventricular white matter (arrows G–J) and corpus callosum (asterisks in G–J). There is, however, decreased overall white matter volume and *ex vacuo* dilatation of the ventricular system and cerebral sulci, likely because of improved brain parenchymal edema and swelling and generalized brain volume loss on subsequent imaging.

has important implications for AAV gene therapy because it could allow repeat dosing. Moreover, the immune modulation regimen used in this study enabled sparing use of glucocorticoids after gene therapy administration.

We hypothesize that combining dual routes of administration of an AAV9-*hASPA* gene transfer therapy with immunomodulators could improve therapeutic outcomes in patients with Canavan disease by increasing vector distribution and restoring ASPA expression in the CNS. Remyelination in the CNS, restoration of visual function, and neurodevelopmental improvement were shown during the first 2 years after AAV dosing, and reduction of NAA accumulation was shown during the first 4 years after AAV dosing.

Further evaluation in a larger cohort of patients is needed to determine the generalizability of this case study; however, our findings suggest that gene therapy could modify or reverse the natural history of Canavan disease. In addition, future studies should consider immunomodulation prior to AAV exposure to enable repeat AAV dosing and prevent immune responses.

MATERIALS AND METHODS
Anti-AAV9 antibody titers
Serum samples from the patient were assayed for circulating antibodies to the AAV9 capsid. Briefly, 96-well plates were coated with 1.2×10^9 AAV9 particles per well in sodium bicarbonate buffer (pH 8.4) overnight at $4°C$. Subsequently, the plates were washed with a solution containing phosphate-buffered saline (PBS) and 0.05% Tween 20 (PBS-T) and then blocked with 10% fetal bovine serum (FBS; Cellgro) for 2 h at $37°C$. After being washed with

PBS-T, the samples were serially diluted from 1:10 to 1:10,240 with a known positive human standard and allowed to bind overnight at $4°C$. The plates were washed again, followed by addition of a secondary antibody (goat anti-human IgG or IgM conjugated with horseradish peroxidase [HRP], Invitrogen) at a dilution of 1:20,000 for 2 h at $37°C$. Finally, the plates were washed and incubated with $3,3',5,5'$-tetramethylbenzidine (TMB) peroxidase substrate (Seracare Life Sciences) in the dark. Reactions were stopped with 0.1 M phosphoric acid. The reaction product was measured by spectrophotometric absorbance at 450 nm using Gen5 Microplate Reader and Imager Software (BioTek Instruments). Sample titers were calculated using the mean absorbance of up to three dilutions that were within the linear region of a 4-parameter logistic standard curve generated by a known positive human standard.

Anti-ASPA antibody titers
Serum samples from the patient were also assayed for circulating antibodies to ASPA. Briefly, 96-well plates were coated with 5 μg/mL recombinant human ASPA protein (Novus Biologicals) per well overnight at $4°C$. The plates were washed three times and then blocked with 10% FBS for 2 h at $37°C$. After being washed 3 more times with PBS-T, 23 negative control samples at a 1:10 dilution and patient samples diluted from 1:10 to 1:20,480 were added and incubated overnight at $4°C$. Each negative control and patient sample were tested in duplicate. The plates were washed three more times, followed by addition of goat anti-human IgG-HRP antibody (Invitrogen) at a dilution of 1:20,000 and incubated for 2 h at $37°C$. Finally, the plates were triple washed with PBS-T and incubated with TMB peroxidase substrate in the dark. Reactions were stopped with 0.1 M phosphoric acid, and their absorbance values were measured at 450 nm. Sample titers were
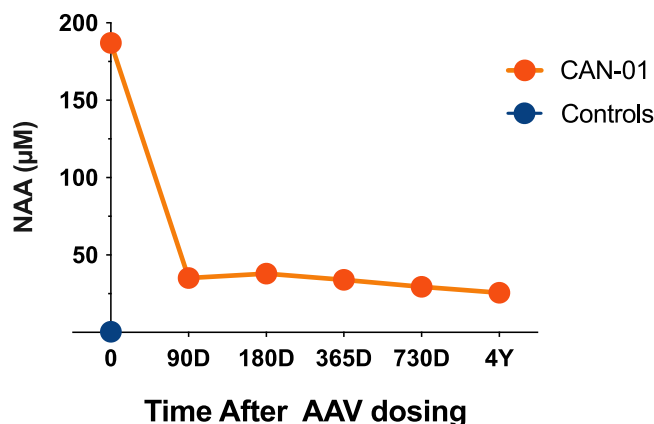
Figure 3. _N_-acetylaspartate (NAA) levels in the cerebrospinal fluid (CSF) of a patient with Canavan disease 0, 90, 180, 365, and 730 days and 4 years after receiving treatment with recombinant adeno-associated virus (AAV) serotype 9-mediated human aspartoacylase (rAAV9-hASPA) gene transfer therapy

NAA levels in CSF samples were assessed by LC-mass spectrometry.

determined by the highest dilution factor with a mean absorbance above the negative cutoff value, which was defined as the mean absorbance of all negative control samples plus three times the standard deviation.

DNA extraction and qPCR

DNA was extracted from whole-blood samples using a DNeasy Blood and Tissue kit (QIAGEN) according to the manufacturer's protocol. DNA was quantified with a NanoDrop One Microvolume UV-visible (UV-vis) spectrophotometer (Thermo Fisher Scientific).

TaqMan qPCR was performed with QuantStudio 3 (Applied Biosystems) using the QuantStudio Design and Analysis Software (v.1.4.1) according to the manufacturer's instructions. A primer and probe set was designed for the chicken β-actin promoter (CB6). Briefly, an 8-log standard curve from $1–10^8$ copies was generated using a stock plasmid containing the CB6 promoter. Threshold cycle (C_t) values for each standard were plotted against the log concentration of copies per sample and analyzed using linear regression, which was used to calculate the number of copies in each sample.

Samples were tested in triplicate, and each replicate was spiked with 10 copies of the target plasmid to test inhibition of the reaction. Each 50-μL reaction contained 25 μL TaqMan Universal PCR Master Mix (Applied Biosystems), up to 0.1 μg sample DNA, 700 nM forward (5′-CATCTACGTATTAGTCATCGCTATTACCA-3′) and reverse (5′-CCCATCGCTGCACAAAATAATTA-3′) primers, and 100 nM probe (6carboxyfluorescein [6FAM]-CCACGTTCTGC TTCACTCTCCCCATC-tetramethylrhodamine [TAMRA]) labeled with a 5′ fluorescent reporter dye (6FAM) and a 3′ fluorescent quencher dye (TAMRA). Cycling was performed according to the manufacturer's guidelines (5 min at 95°C for initial denaturation

and enzyme activation, followed by 45 cycles alternating between 15 s at 95°C for denaturing and 60 s at 60°C for annealing and extension). Results were averaged across two replicates and normalized to vector genome copies per microgram of DNA.

Vector generation

The design of the study agent (rAAV9-CB6-_hASPA_) has been described previously.[12] Briefly, the rAAV9 vector contains a modified chicken β-actin (CB6) promoter and the human _ASPA_ (_hASPA_) gene, which was codon optimized and included a Kozak sequence. After preclinical development and validation studies at UMass, the study agent was manufactured at the Human Applications Laboratory, Powell Gene Therapy Center at UF.

Gene therapy administration

I.v. and i.c.v. infusions of rAAV9-CB6-_hASPA_ were performed as an inpatient procedure at Shands Children's Hospital (Gainesville, FL, USA) in April 2017 on study day 0. The i.v. dose administered was 4.5×10^{13} vector genomes (vg) per kg body weight in 12 mL PBS, and the total i.c.v. dose was 5.0×10^{13} vg in 2 mL PBS. The patient's weight was 10 kg, so the total vector dose was 5×10^{14} vg.

During the i.c.v. procedure, a ventriculostomy catheter and an external ventricular drainage (EVD) catheter were placed using Image Fusion 3D MRI guidance under anesthesia. The patient was discharged the day after the procedure without complications.

Immunomodulation

To reduce immune responses to the vector capsid and transgene, the patient received 750 mg/m² rituximab (Genentech) i.v. prior to AAV9 infusion on study days −15 and −3 and 375 mg/m² on study day 180. In addition, from the second rituximab administration (study day −3) until study day 360, the patient received 0.6 to 1 mg/m²/day sirolimus (Wyeth Pharmaceuticals) orally, adjusted to maintain a trough serum concentration of 3–7 ng/mL. The patient was also treated with solumedrol (1 mg/kg) on study day 0 and oral prednisolone (1 mg/kg/day) on study days 3 and 5.

The patient also received IVIG on study day 180, when serum immunoglobulin levels decreased below 700 mg/dL, to maintain sufficient protection against infectious agents.

Motor evaluation

An experienced clinical evaluator tested the child at baseline and on days 270, 365, 520, and 730. The following scales were used.

GMFM

The GMFM is a criterion-referenced outcome measure that looks at 5 subsets of movement (lying and rolling, sitting, crawling and kneeling, standing, and walking/running/jumping). It is based on an ordinal (0–3) scale. Compensatory patterns are allowed to achieve a score of 3 as it looks at functional task completion and not specifically at quality of movement. It has been validated on children
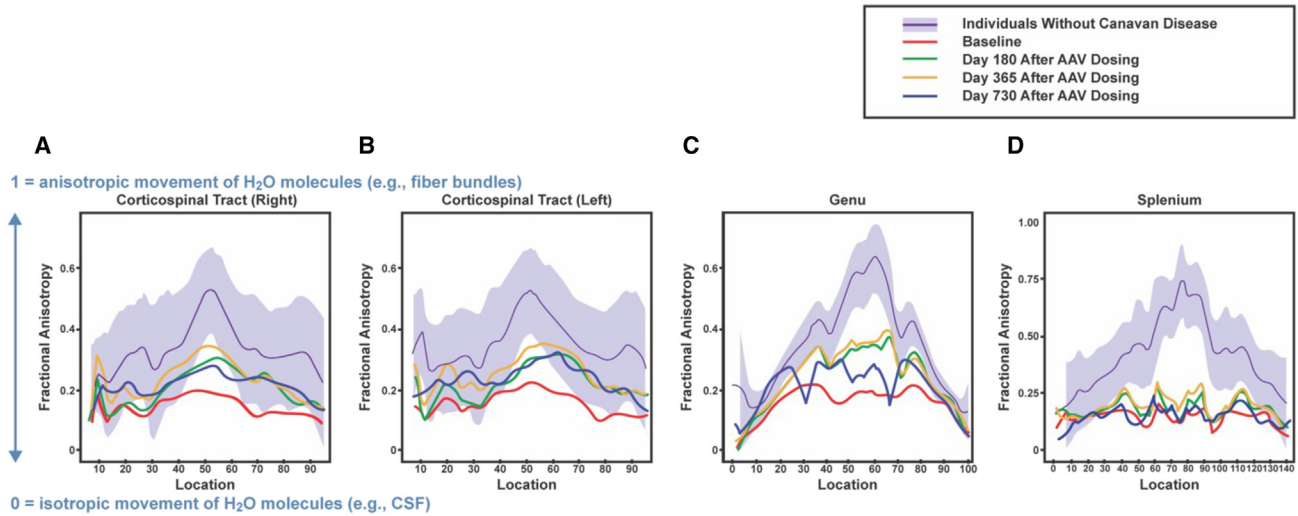
Figure 4. Fractional Anisotropy (FA) measurements in the brain in a patient with Canavan disease pre and post gene transfer therapy
(A and B) FA values in the right and left corticospinal tracts. (C and D) FA values in the anterior (genu) and posterior (splenium) corpus callosum. Red, green, orange, and blue lines indicate FA values at baseline and 180, 365, and 730 days after rAAV9-hASPA administration, respectively. Purple lines and shaded purple areas represent means and standard deviations for 400 individuals without Canavan disease between birth and 3 years of age. On the y axis, FA ranges from 0 (isotropic movement of water molecules [e.g., in CSF]) to 1 (anisotropic movement of water molecules [e.g., in fiber bundles]). The numbers on the x axis indicate the relative distance from the central axis of the corticospinal tract (i.e., higher values are more peripheral). AAV, adeno-associated virus; CSF, cerebrospinal fluid.

with cerebral palsy and Down syndrome (5 months to 16 years) and has been used in child and adult Pompe clinical trials for the past decade.[32–34]

CHOP-INTEND
CHOP-INTEND is a reliable measure of motor skills for untreated infants with spinal muscular atrophy (SMA) from 0–2 years of age and other neuromuscular disorders that present in infancy.[17]

MFM-20 and MFM-32
These tests provide a numerical measure of the static and dynamic motor capacity of a subject with a neuromuscular disorder. It measures 3 domains: standing and transfers, axial and proximal motor function, and distal motor function. The MFM-20 and -32 are sensitive to change in patients with DMD and SMA and may be useful in other rare disease populations that experience progressive muscle weakness.[18]

Bayley Scales of Infant and Toddler Development, Third Edition (Bayley-III)
Bayley-III is a norm-referenced outcome measure for 1–42 months in domains of cognition, receptive language, expressive language, fine motor, and gross motor skills.[35]

MRI
Baseline and follow-up (days 90, 180, 365, and 730) imaging were performed under general anesthesia on a 3T MR unit (Verio, Siemens, Erlangen, Germany) by using a routine pediatric brain MR protocol in our institution. The parameters for the T1W imaging were as follows: repetition time (TR), 250 ms; echo time (TE), 2.71 ms; field of view

(FOV), 190 × 190 mm^2; flip angle = 70°; slice thickness, 4 mm. The parameters for the T2W imaging were as follows: TR, 4,600 ms; TE, 125 ms; FOV, 190 × 190 mm^2; flip angle = 90°; slice thickness, 4 mm. MRS was obtained with a TE of 135 ms from the voxels in the right and left frontal white matter as well as from the voxels in the phantoms on both sides of the head. In addition, 64 directional DTIs were performed with the following parameters: b value: 1,000 s/mm^2; TR, 17,300 ms; TE, 81 ms; FA, 90°; slice thickness, 2 mm. It is known in the literature that, on conventional imaging, mature myelin is hyperintense to the gray matter cortex on T1 and hypointense to the gray matter cortex on T2.[20] We use our conventional anatomical imaging of T1 and T2 weighted imaging to qualitatively evaluate change in white matter signal in assessment of myelin formation and maturation on follow-up imaging.

Controls for DTI were generated from healthy children from data shared by NIH grant "DTI as a tool to identify infants with Krabbe disease in need of urgent treatment" (funding agency: NIH/NINDS 1R01NS061965-01, investigator,: M.L.E.).

CSF collection
The child was positioned in the customary side-lying position to obtain CSF samples. A 22G spinal needle was inserted into the subarachnoid space at the L3-L4 level at the time of MRI studies were general anesthesia was administered.

NAA evaluation by mass spectrometry
NAA extraction
50 μL of CSF was spiked with 2 ng of NAA internal standard (13C4-NAA) in 50 μL of 5% sulfosalicylic acid (SSA). 400 μL
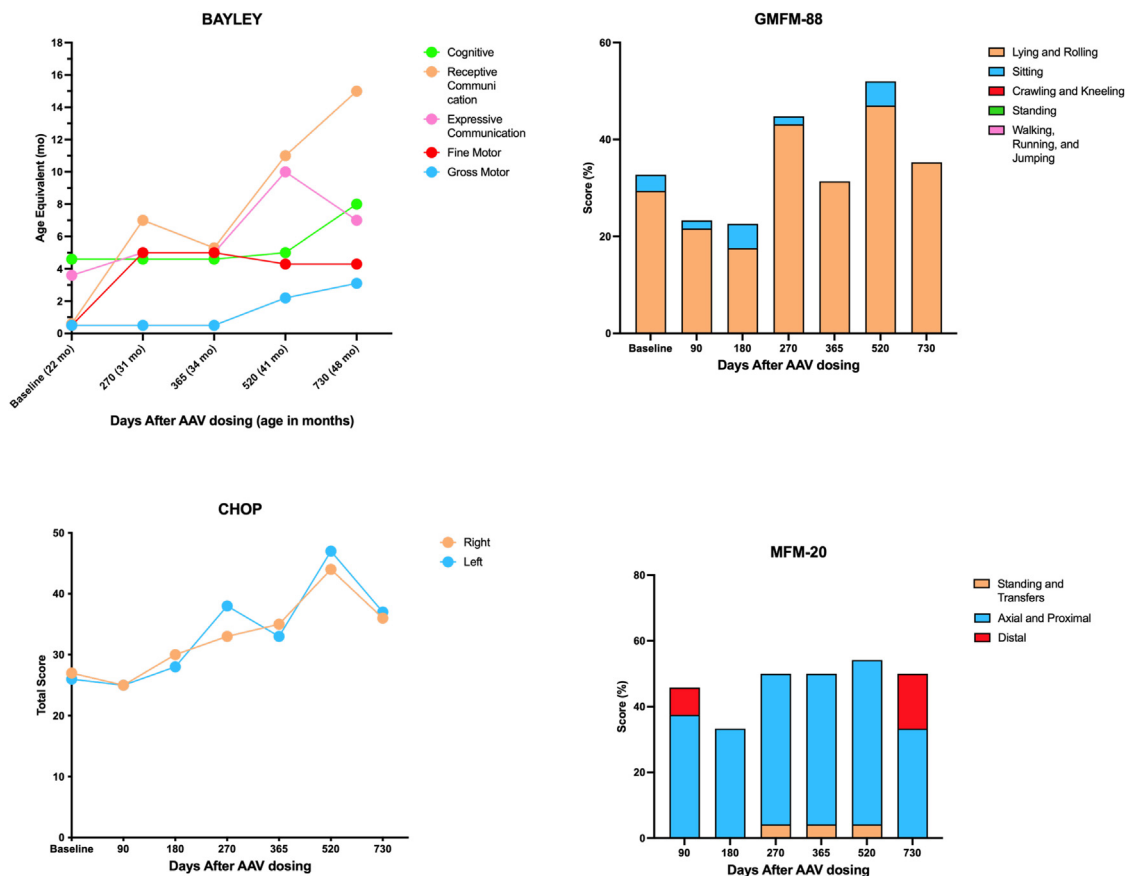
Figure 5. Motor development in a patient with Canavan disease pre and post gene transfer therapy

Changes in the Bayley Scale of Infant and Toddler Development, Gross Motor Function Measure 88 (GMFM-88), Children's Hospital of Philadelphia Infant Test of Neuromuscular Disorders (CHOP INTEND), and Motor Function Measure Short Form (MFM-20) child development assessment scales, respectively, after administration of rAAV9-hASPA.

cold methanol was added to each sample, and the samples were pulse sonicated in ice with a sonic dismembranator (Thermo Fisher Scientific, Waltham, MA, USA) for 30 s, incubated on ice for 10 min, and then pulsed again for 30 s. Samples were pelleted by centrifugation at $6,000 \times g$ for 5 min at room temperature. 500 µL of supernatant was moved to a clean microcentrifuge tube, dried down under nitrogen, and re-suspended in 50 µL of 5% (w/v) SSA in water. 3-µL injections were used for liquid chromatography (LC)-HRMS analysis. The calibration curve was constructed in methanol, using concentrations between 0.2 and 25 ng/ µL authentic NAA and same amount of internal standard as for the real samples. The calibration equation was as follows: $y = 0.143 \times +0.01$ with R2 = 0.9997. The quality control samples were within ±3%. All measurements were done in triplicate injections with a coefficient of variability of under 2%.

Metabolomic LC-HRMS

NAA was separated from other metabolites using a method similar to Guo et al.,[36] using an XSelect HSS C18 column (2.1 × 150 mm,

3.5-µm particle size) (Waters, Milford, MA, USA) in an UltiMate 3000 quaternary UHPLC (Thermo Fisher Scientific) equipped with a refrigerated autosampler (5°C) and column heater (50°C). Solvent A consisted of water with 5 mM DIPEA and 200 mM HFIP, and solvent B consisted of MeOH with 5 mM DIPEA and 200 mM HFIP. Flow gradient conditions were as follows: 0% B for 6 min at 0.18 mL min^{-1}, increased to 1% B for 2 min at 0.2 mL min^{-1}, increased to 2% B for 4 min, increased to 14% B for 2 min, increased to 70% B for 2 min, increased to 99% B for 1 min, increased flow rate to 0.3 mL min^{-1} for 0.5 min, increased flow rate to 0.4 mL min^{-1} for 4 min, then washed by decreasing to 0% B for 2.3 min at 0.3 mL min^{-1}, decreased to 0.2 mL min^{-1} for 0.2 min, and ending with flow of 0.18 mL min^{-1}. Retention time was 7.8 min for NAA and its internal standard. Samples were analyzed using a Q Exactive HF (QE-HF) (Thermo Fisher Scientific) equipped with a heated electrospray ionization (HESI) source operated in negative ion mode exactly as described by Frederick et al.[37] Column effluent was diverted to the QE-HF from 0.5– 19 min and then to waste for the remaining time of the run. Data analysis was done using Xcalibur 4.2 (Thermo Fisher Scientific)
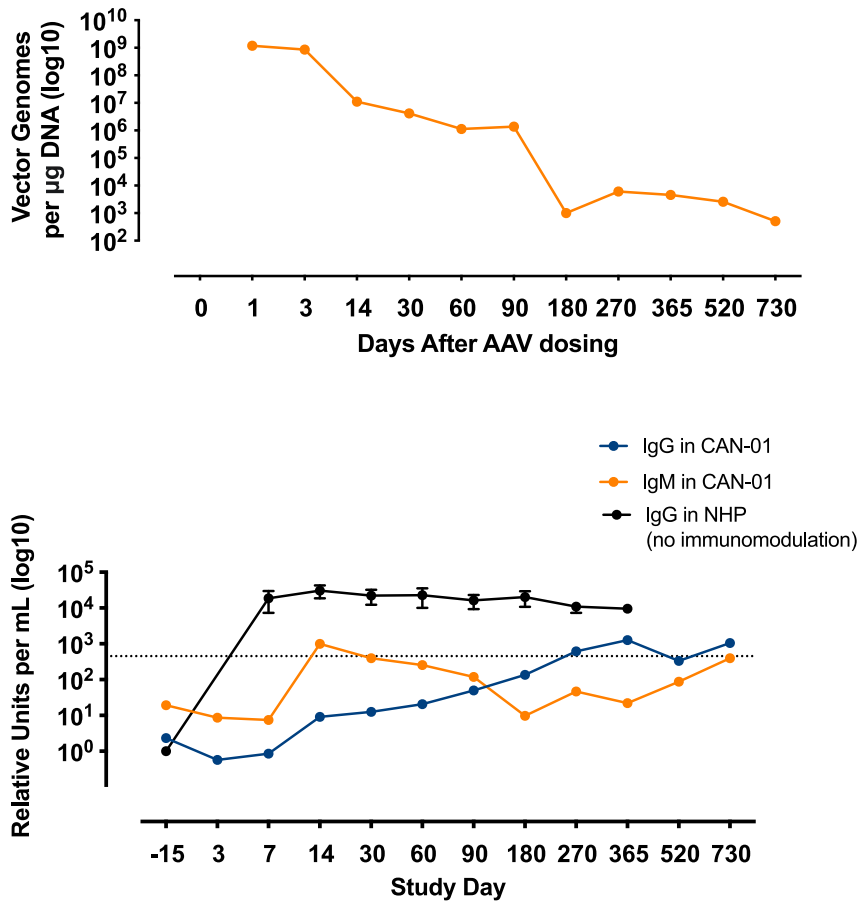
Figure 6. Vector genomes and anti-AAV9 antibody levels in a patient with Canavan disease pre and post gene transfer therapy

Top panel: the concentration of vg in peripheral blood after administration of rAAV9-hASPA gene transfer therapy (study day 0). Bottom panel: the levels of anti-AAV9 IgG (blue line) and IgM (orange line) in serum during the study. The patient received rituximab on study days −15, −3, and 180, and IV immunoglobulin on study day 180. IgG, immunoglobulin G; IgM, immunoglobulin M; NHP, nonhuman primate.

from the full scan data at 120,000 resolution (174.0404 for NAA and 178.0538 for its internal standard).

Vector manufacturing

AAV9-CB6-hAspA was produced in a campaign mode in compliance with cGMP in the Human Applications Laboratory at UF (Gainesville, FL, USA). The vector was produced in HEK293 cells using a co-transfection procedure. After expansion of HEK293 cells, which originate from a working cell bank, into 10-layer CellSTACKS, cells were co-transfected using a $CaPO_4$ precipitation method with the helper and vector plasmids (pTR-UF9-KanR and pTR-CB6-AspA). After approximately 72 h, cells were harvested. The rAAV9-CB6-ASPA Harvest was frozen and stored. To continue processing, the cell harvest was thawed and resuspended in WFI and 100 mM sodium citrate buffer with Benzonase. After 1-h incubation at 37°C, the cell suspension was divided into four equal parts, and 100 mM citric acid and WFI were added, mixed, and then centrifuged at 4,000 rpm for 10 min. The supernatant was then purified by SP chromatography. Peak fractions were collected after elution with a 40% solution of sodium citrate/citric acid elution buffer B in sodium citrate/citric acid wash buffer A. The purified bulk peak was then sterile filtered. In-process testing was performed on harvests and purified

pulk. The purified bulks that met set specifications were concentrated using a 5-mL SP HiTrap column. Peak fractions were collected after elution with a 40% solution of sodium citrate/citric acid elution buffer B in sodium citrate/citric acid wash buffer A. The concentrated bulk peak was then sterile filtered. Concentrated bulks were combined into one container, sterile filtered, and then vialed. Final product testing was performed on randomly selected final product vials. A total of seven final product vials were thawed, pooled, and dialyzed against DPBS. Following dialysis, a single product vial was filled.

DATA AVAILABILITY

All original data are available from the authors by request.

AUTHOR CONTRIBUTIONS

DECLARATION OF INTERESTS

REFERENCES

1. Kaul, R., Gao, G.P., Balamurugan, K., and Matalon, R. (1993). Cloning of the human aspartoacylase cDNA and a common missense mutation in Canavan disease. Nat. Genet. 5, 118–123.

2. Bokhari, M.R., Samanta, D., and Bokhari, S.R.A. (2021). Canavan Disease. StatPearls. Treasure (StatPearls Publishing).

3. Leone, P., Shera, D., McPhee, S.W.J., Francis, J.S., Kolodny, E.H., Bilaniuk, L.T., Wang, D.J., Assadi, M., Goldfarb, O., Goldman, H.W., et al. (2012). Long-term follow-up after gene therapy for canavan disease. Sci. Transl. Med. 4, 165ra163.

4. Moffett, J.R., Ross, B., Arun, P., Madhavarao, C.N., and Namboodiri, A.M.A. (2007). N-Acetylaspartate in the CNS: from neurodiagnostics to neurobiology. Prog. Neurobiol. 81, 89–131.

5. Bley, A., Denecke, J., Kohlschütter, A., Schön, G., Hischke, S., Guder, P., Bierhals, T., Lau, H., Hempel, M., and Eichler, F.S. (2021). The natural history of Canavan disease: 23 new cases and comparison with patients from literature. Orphanet J. Rare Dis. 16, 227.

6. Hoshino, H., and Kubota, M. (2014). Canavan disease: clinical features and recent advances in research. Pediatr. Int. 56, 477–483.

7. Janson, C., McPhee, S., Bilaniuk, L., Haselgrove, J., Testaiuti, M., Freese, A., Wang, D.J., Shera, D., Hurh, P., Rupin, J., et al. (2002). Clinical protocol. Gene therapy of Canavan disease: AAV-2 vector for neurosurgical delivery of aspartoacylase gene (ASPA) to the human brain. Hum. Gene Ther. 13, 1391–1412.

8. Leone, P., Janson, C.G., Bilaniuk, L., Wang, Z., Sorgi, F., Huang, L., Matalon, R., Kaul, R., Zeng, Z., Freese, A., et al. (2000). Aspartoacylase gene transfer to the mammalian central nervous system with therapeutic implications for Canavan disease. Ann. Neurol. 48, 27–38.

9. Ingusci, S., Verlengia, G., Soukupova, M., Zucchini, S., and Simonato, M. (2019). Gene therapy tools for brain diseases. Front. Pharmacol. 10, 724.

10. Ahmed, S.S., Li, H., Cao, C., Sikoglu, E.M., Denninger, A.R., Su, Q., Eaton, S., Liso Navarro, A.A., Xie, J., Szucs, S., et al. (2013). A single intravenous rAAV injection as late as P20 achieves efficacious and sustained CNS Gene therapy in Canavan mice. Mol. Ther. 21, 2136–2147.

11. Ahmed, S.S., and Gao, G. (2015). Making the White Matter Matters: Progress in Understanding Canavan's Disease and Therapeutic Interventions Through Eight Decades. JIMD Rep. 19, 11–22.

12. Gessler, D.J., Li, D., Xu, H., Su, Q., Sanmiguel, J., Tuncer, S., Moore, C., King, J., Matalon, R., and Gao, G. (2017). Redirecting N-acetylaspartate metabolism in the central nervous system normalizes myelination and rescues Canavan disease. JCI Insight 2, e90807.

13. Gessler, D.J., Lotun, A., Bi, S., and Gao, G. (2020). Disease specific neurometabolic pathways are corrected in an age-dependent manner independent of rAAV gene delivery efficacy. Mol. Ther. 28, 318.

14. Foust, K.D., Nurre, E., Montgomery, C.L., Hernandez, A., Chan, C.M., and Kaspar, B.K. (2009). Intravascular AAV9 preferentially targets neonatal neurons and adult astrocytes. Nat. Biotechnol. 27, 59–65.

15. Corti, M., Liberati, C., Smith, B.K., Lawson, L.A., Tuna, I.S., Conlon, T.J., Coleman, K.E., Islam, S., Herzog, R.W., Fuller, D.D., et al. (2017). Safety of intradiaphragmatic delivery of adeno-associated virus-mediated alpha-glucosidase (rAAV1-CMV-hGAA) gene therapy in children affected by Pompe disease. Hum. Gene Ther. Clin. Dev. 28, 208–218.

16. Balasundaram, P., and Avulakunta, I.D. (2021). Bayley Scales of Infant and Toddler Development. StatPearls. Treasure (StatPearls Publishing).

17. Glanzman, A.M., Mazzone, E., Main, M., Pelliccioni, M., Wood, J., Swoboda, K.J., Scott, C., Pane, M., Messina, S., Bertini, E., et al. (2010). The Children's Hospital of Philadelphia Infant Test of Neuromuscular Disorders (CHOP INTEND): test development and reliability. Neuromuscul. Disord. 20, 155–161.

18. de Lattre, C., Payan, C., Vuillerot, C., Rippert, P., de Castro, D., Bérard, C., and Poirot, I.; MFM-20 Study Group (2013). Motor function measure: validation of a short form for young children with neuromuscular diseases. Arch. Phys. Med. Rehabil. 94, 2218–2226.

19. Harvey, A.R. (2017). The Gross Motor Function Measure (GMFM). J. Physiother. 63, 187.

20. Branson, H.M. (2013). Normal myelination: a practical pictorial review. Neuroimaging Clin. 23, 183–195.

21. Gilmore, J.H., Lin, W., Corouge, I., Vetsa, Y.S.K., Smith, J.K., Kang, C., Gu, H., Hamer, R.M., Lieberman, J.A., and Gerig, G. (2007). Early postnatal development of corpus callosum and corticospinal white matter assessed with quantitative tractography. AJNR. Am. J. Neuroradiol. 28, 1789–1795.

22. Grotheer, M., Rosenke, M., Wu, H., Kular, H., Querdasi, F.R., Natu, V.S., Yeatman, J.D., and Grill-Spector, K. (2022). White matter myelination during early infancy is linked to spatial gradients and myelin content at birth. Nat. Commun. 13, 997.

23. Pardridge, W.M. (2005). The blood-brain barrier: bottleneck in brain drug development. NeuroRx 2, 3–14.

24. Hudry, E., and Vandenberghe, L.H. (2019). Therapeutic AAV gene transfer to the nervous system: a clinical reality. Neuron 101, 839–862.

25. Taghian, T., Marosfoi, M.G., Puri, A.S., Catalepe, O.I., King, R.M., Diffie, E.B., Maguire, A.S., Martin, D.R., Fernau, D., Batista, A.R., et al. (2020). A safe and reliable technique for CNS delivery of AAV vectors in the cisterna magna. Mol. Ther. 28, 411–421.

26. Pardridge, W.M. (2019). Blood-brain barrier and delivery of protein and gene therapeutics to brain. Front. Aging Neurosci. 11, 373.

27. Cohen-Pfeffer, J.L., Gururangan, S., Lester, T., Lim, D.A., Shaywitz, A.J., Westphal, M., and Slavc, I. (2017). Intracerebroventricular delivery as a safe, long-term route of drug administration. Pediatr. Neurol. 67, 23–35.

28. Scott DW, Rouse JL, Romero KB, Eclov R, Lewis TEW, Kapadia M, Mansfield G, Beard CW, editors. A route of administration study of BBP-812, an AAV9-based gene therapy for the treatment of Canavan disease, in juvenile cynomolgus macaques. European Society of Gene and Cell Therapy 27th Annual Congress; October 22-25, 2019; Barcelona, Spain.

29. Hordeaux, J., Tuske, S., Yu, T.W., So, M., Tsai, P., Bell, P., Gotschall, R.R., Do, H., and Wilson, J.M. (2020). Combined CNS and systemic directed gene therapy in a mouse model of Pompe disease with advanced disease at treatment. Mol. Ther. 28, 403.

30. Pipe, S., Leebeek, F.W.G., Ferreira, V., Sawyer, E.K., and Pasi, J. (2019). Clinical considerations for capsid choice in the development of liver-targeted AAV-based gene transfer. Mol. Ther. Methods Clin. Dev. *15*, 170–178.

31. Calcedo, R., and Wilson, J.M. (2013). Humoral immune response to AAV. Front. Immunol. *4*, 341.

32. Beckers, L.W.M.E., and Bastiaenen, C.H.G. (2015). Application of the Gross Motor Function Measure-66 (GMFM-66) in Dutch clinical practice: a survey study. BMC Pediatr. *15*, 146.

33. Hanna, S.E., Bartlett, D.J., Rivard, L.M., and Russell, D.J. (2008). Reference curves for the Gross Motor Function Measure: percentiles for clinical description and tracking over time among children with cerebral palsy. Phys. Ther. *88*, 596–607.

34. Ko, J., and Kim, M. (2013). Reliability and responsiveness of the gross motor function measure-88 in children with cerebral palsy. Phys. Ther. *93*, 393–400.

35. Del Rosario, C., Slevin, M., Molloy, E.J., Quigley, J., and Nixon, E. (2021). How to use the Bayley Scales of Infant and Toddler Development. Arch. Dis. Child. Educ. Pract. Ed. *106*, 108–112.

36. Guo, L., Wang, Q., Weng, L., Hauser, L.A., Strawser, C.J., Rocha, A.G., Dancis, A., Mesaros, C., Lynch, D.R., and Blair, I.A. (2018). Liquid Chromatography-High Resolution Mass Spectrometry Analysis of Platelet Frataxin as a Protein Biomarker for the Rare Disease Friedreich's Ataxia. Anal. Chem. *90*, 2216–2223.

37. Cai, K., Frederick, R.O., Tonelli, M., and Markley, J.L. (2018). Interactions of iron-bound frataxin with ISCU and ferredoxin on the cysteine desulfurase complex leading to Fe-S cluster assembly. J. Inorg. Biochem. *183*, 107–116.